JPE 16-4-33

http://dx.doi.org/10.6113/JPE.2016.16.4.1598
ISSN(Print): 1598-2092 / ISSN(Online): 2093-4718

The Optimized Design of a NPC Three-Level Inverter Forced-Air Cooling System Based on Dynamic Power-loss Calculations of the Maximum Power-Loss Range

Shi-Zhou Xu* and Feng-You He†

*,†Dept. of Information and Electrical Eng., China University of Mining and Technology, Xuzhou, China

Abstract

In some special occasions with strict size requirements, such as mine hoists, improving the design accuracy of the forced-air cooling systems of NPC three-level inverters is a key technology for improving the power density and decreasing the volume. First, a fast power-loss calculation method was brought. Its calculation principle introduced in detail, and the computation formulas were deduced. Secondly, the average and dynamic power losses of a 1MW mine hoist acting as the research target were analyzed, and a forced-air cooling system model based on a series of theoretical analyses was designed with the average power loss as a heat source. The simulation analyses proves the accuracy and effectiveness of this cooling system during the unit lifting period. Finally, according to an analysis of the periodic working condition, the maximum power-loss range of a NPC three-level inverter under multi cycle operation was obtained and its dynamic power loss was taken into the optimized cooling system model as a heat source to solve the power device damage caused by instantaneous heat accumulation. The effectiveness and feasibility of the optimization design based on the dynamic power loss calculation of the maximum power-loss range was proved by simulation and experimental results.

Key words: Cooling system, Heat sink optimization, NPC three-level inverter, Power loss calculation

I. INTRODUCTION

In recent years, the application of NPC three-level inverters has been increasing gradually with the increasing capacity of mine hoists. As a special application, the mine hoist working conditions are particular and complex due to their limited space, which requires a much higher power density from the inverter. In terms of the entire inverter system, the cooling system occupies a large space and its size plays an important role in improving power density. Therefore, the research object of this article is the forced-air cooling system of three-level inverters, and the research goal is to optimize the cooling system into an effective and accurate one with a maximum power density and a minimum volume. This is done based on the maximum power loss calculation of the interval dynamic loss.

As shown in [1], about 60% of inverter failures are caused by high temperatures, and a double failure rate comes out with every 10℃of increase. Therefore, on the basis of an accurate power loss calculation of the power devices in an inverter, it becomes possible and necessary to design an efficient cooling system to improve the thermal stability of the whole system. However, if an accurate analysis and design of the cooling system need to be obtained, the premise is to calculate the inverter power loss accurately. Until now, some research has been done by a number experts and scholars. Currently, there are many studies on power-loss calculations and thermal analysis for single IGBT modules and two-level inverters[2]-[6]. That[7]-[10] did not consider the impact of the junction temperature of power devices on power losses, is the main reason for errors between their theoretical calculations and experimental results. Dieckerhoff [10] considered that the switching power loss of power

Manuscript received Nov. 19, 2015; accepted Mar. 9, 2016
Recommended for publication by Associate Editor Sang-Won Yoon.
†Corresponding Author: xushizhousiee@163.com
Tel: +86-15062190287, Fax: +86-0516-80139933, China Univ. of Mining & Tech.
*Dept. of Information and Electrical Eng., China Univ. of Mining and Tech., China

devices has a linear relationship with withstanding voltage. However, this assumption is approximately valid only in the ±20% range of the test voltage. A very accurate loss calculation and heat dissipation method was introduced in [11]. However, it did not take all of the heat sources into consideration. This has an effect on the power devices and thermal analysis. In [12], the transient modeling of the losses and thermal dynamics in power semiconductor devices is analyzed. However, the model needs to be improved by considering the peripheral circuits. In [13], it has been proposed that the power losses of inverters can be calculated by simulating a model of the power devices. However, the model was built on the basis of actual operation conditions and an analysis of each power device. Some conducting loss calculation methods for the IGBTs and diodes of inverters were presented in [13] and [14]. All of them were completed by using the on-state voltage drop, current and duty cycle to do the caluclations. For switching losses, a much more direct way is through a large number of repeated trials, where a great deal of test data can be collected. Then approximate data can be obtained based on various effecting factors through curve fitting. Even though this is an easy way to calculate, the results can be easily affected by different experimental conditions. A much more accurate method is cutting the switching process of power devices into several stages and calculating each stage's power loss by the integral [9], [15].However, the value of this calculation method is the average power loss of the inverter, which is not suitable for a hoist with a very large overload coefficient at different sections of the whole operation cycle. In [16], Xiang-ning He proposed an approximate on-line model of inverter power loss based on an IGBT off-line test platform. With this model the commutation mode, modulation method and load type of inverters can be equaled. On the basis of this, the total power losses at different junction temperatures can be obtained, and after interpolation calculations, the power loss at a certain temperature can be obtained. Even though this method can get a more accurate power loss under certain temperatures, the results are an average total power loss under a certain temperature and cannot meet aperiodic load with a large instantaneous overcurrent. From what has been stated above, all of the former methods are only valid for inverters under normal working conditions. For high power mine hoists, they have very large overload currents in the acceleration and deceleration periods in a short time. In addition, the instantaneous total power loss within these ranges is very large. This range is composed by the deceleration period of the former cycle and the acceleration period of the latter period is the so called the maximum power range. However, during the constant velocity range, the power loss is much less and can spread evenly during a much longer period. Even though the huge heat generated during this range is weakened for an inverter working in only one cycle or in many cycles

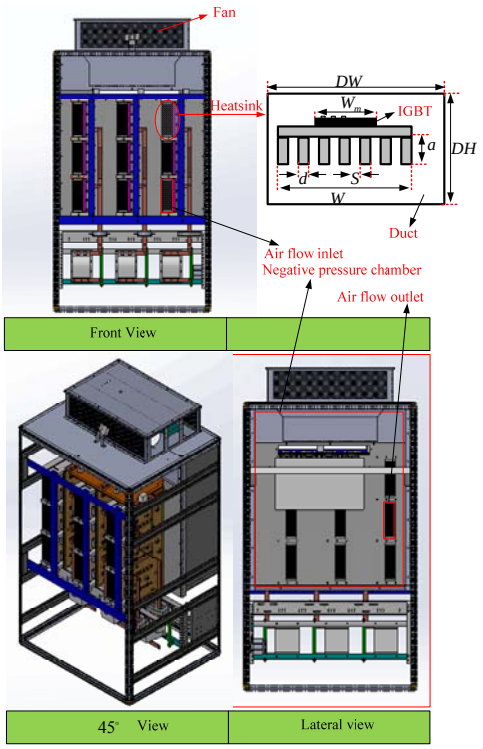

Fig. 1. Forced-air cooling system structure of NPC three-level inverter.

with long intervals, and cannot affect the inverter under this condition, for those inverters under multicycle operation with no intervals or only a little interval, it results in lethal damage. When using the above methods to calculate the total power loss in one cycle as a heat source to de sign anair-forced cooling system, the heat accumulation phenomenon caused by a large power loss in the maximum power range is covered by a small average value with a long cooling period. This covers the actual capacity of the cooling system and causes serious damage to mine hoists under special operating conditions. Therefore, in this paper, according to the mine hoist operating condition, the maximum power range was extracted to calculate the dynamic power loss of a NPC three-level inverter as a heat source to optimize the design of a forced-air cooling system.

At present, many studies have been done on the forced-air cooling system designs in inverters, and the axial flow induced draft fan is one of the most common styles as a research object. In accordance with the installation position, this style can be divided into overhead and knapsack types. Both of these typeshave their own advantages in terms of space saving. The research object of this paper is overhead cooling, whose structure is shown in Fig. 1. It is indicatedin [17] and [18]that empirical formulas and analysis models have been alternative methods to describe many models accurately, and the authors have discussed the theory power limit of a converter system to optimize a heat sink. A fin type array of forced convection cooling plates was

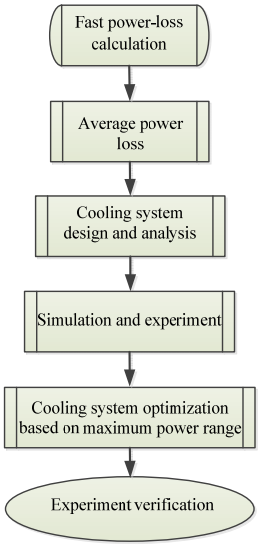

Fig. 2. Flow chart of cooling system optimization based on maximum power-loss range.

described in [19]. A practical guidance forselecting a heat sink was given in [20], and some design processes were recommended as well. Leonard et al. summarized the bypass flow characteristics in plate-fin heat sinks and put forward their design model to calculate the bypass flow [21]. For the purpose of accurately calculating bypass flow, Hossain et al. [22] proposed a comprehensive analysis process and deduced a simple empirical equation, which can achieveenough analysis and design precision. In this paper, the main work is to use the previously calculated power loss as a heat source to build anaccurate model of a forced-air cooling system and to analyze the cooling capacity. This determines the thermal capacity of the fan, and makes it possible tooptimize the whole system.

Aflow chart is shown in Fig. 2. First, this paper proposed a fast power-loss calculation method to calculate the total average power loss of the NPC three-level inverter in Section II. The cooling system was analyzed and designed using the average power loss as a heat source in Section III. Then the experiment demonstratedthe disadvantages of the average power loss acting as a heat source,while using the maximum power range based on the dynamic power loss calculation of a NPC three-level inverter under dynamic conditions to optimize the design in Section IV. Finally, simulation and experimental results verifies the feasibility and effectiveness of the proposed optimization.

II. Dynamic Power Loss Calculation of NPC Three-Level Inverters

The topology structure of a back-to-back NPC three-level converter is shown in Fig. 3. It can be divided into the NPC-rectifier and the NPC-inverter parts, and the main research object of this paper is the latter.

The power devices used in this topology are IGBTs and

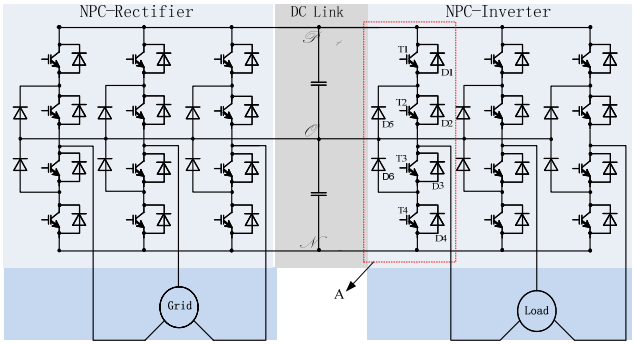

Fig. 3. The topology of back-to-back NPC three-level converter.

diodes, and the power losses of the IGBT P_T include conduction loss P_{cond-T} and switching loss P_{sw_T}.

$$P_T = P_{cond-T} + P_{sw\_T} \tag{1}$$

The power losses of fast recovery diodes P_D consist of conduction loss P_{cond-D} and switching loss P_{sw_D}, namely

$$P_D = P_{cond-D} + P_{sw\_D} \quad . \tag{2}$$

(1) Conduction loss: Due to the existence of an initial saturation voltage drop and conduction resistance, power devices generate conduction losses in the process of conduction. Meanwhile, both the initial saturation voltage drop and conduction resistance change linearly with temperature, and for IGBTs with a fast recovery diode, theconduction properties can be described approximately in the following linear formula:

$$\begin{aligned} v_{CE} &= [r_{ce\_25℃} + K_{r\_T}(T_{j\_T} - 25℃)]i \\ &+[V_{ce\_25℃} + K_{V\_T}(T_{j\_T} - 25℃)] \end{aligned} \tag{3}$$

$$\begin{aligned} v_F &= [r_{F\_25℃} + K_{r\_D}(T_{j\_D} - 25℃)]i \\ &+[V_{F\_25℃} + K_{V-D}(T_{j-D} - 25℃)] \end{aligned} \tag{4}$$

In (3) and (4), v_{CE} and v_F stand for the actual voltage drops of anIGBT and a fast recovery diode, respectively; T_{j_T} and T_{j_D} are the actual junction temperatures of anIGBT and a fast recovery diode, respectively; and K_{r_T} is the temperature coefficient of the temperature impacting on the conduction resistance of an IGBT. K_{r_D} is the temperature coefficient of the temperature impacting on the conduction resistance of a fast recovery diode; K_{V_T} is the temperature coefficient of the temperature impacting on the voltage drop of an IGBT; K_{V-D} is the temperature coefficient of the temperature impacting on the voltage drop of a fast recovery diode; and i is the output current of an inverter.

The fundamental waves of the output AC voltage of an inverter using PWM can be expressed as follows:

$$u = \sqrt{2}U_{out}\cos\theta \tag{5}$$

where, U_{out} is the root mean square of the actual voltage and θ is the phase angle.

When the switching frequency is high enough, the output current i can be approximately equivalent to a sinusoidal current.

$$i = \sqrt{2} I_{out} \cos(\theta - \varphi). \tag{6}$$

In (6), I_{out} is the root mean square of the actual current; φ is the phase angle between the actual current and the actual voltage.

The duty cycle of the given PWM method is as follows:

$$\xi = \frac{1 + M\cos\theta}{2}. \tag{7}$$

In (7), M is the modulation of the PWM (the peak value of the phase voltage divided by 1/2 of the DC voltage of the bridge arm). Under a constant frequency, the duty cycle can be simplified as afunction of the phase angle θ.

In accordance to(3) and (4), the conduction power losses of an IGBT and a fast recovery diode with a sinusoidal output current can be deduced as follows.

$$\begin{aligned} P_{cond-T} &= I_{out}\sqrt{2}\left(\frac{1}{2\pi} + \frac{M\cos\varphi}{8}\right)[V_{ce\_25℃} \\ &+ K_{V\_T}(T_j - 25℃)] + {I_{out}}^2 2\left(\frac{1}{8} + \frac{M\cos\varphi}{3\pi}\right) \\ &\times [r_{ce\_25℃} + K_{r\_T}(T_j - 25℃)] \end{aligned} \tag{8}$$

$$\begin{aligned} P_{cond-D} &= I_{out}\sqrt{2}\left(\frac{1}{2\pi} - \frac{M\cos\varphi}{8}\right)[V_{F\_25℃} \\ &+ K_{V\_D}(T_j - 25℃)] + {I_{out}}^2 2\left(\frac{1}{8} - \frac{M\cos\varphi}{3\pi}\right) \\ &\times [r_{F\_25℃} + K_{r\_D}(T_j - 25℃)] \end{aligned} \tag{9}$$

In (8) and (9), P_{cond-T} and P_{cond-D} are the conduction power losses of an IGBT and a fast recovery diode,respectively.

(2) Switching loss: Switching loss comes from the process of switching on and off. Under special test conditions, the power losses of switching on and switching off can be obtained indirectly by integrating the product of the voltage and current to time, during which the differences between the actual current/voltage and the reference current/voltage must be taken into consideration. In one switching cycle, the switching losses of an IGBT and a fast recovery diode can be represented as:

$$\begin{aligned} P_{sw\_T} &= f_s(E_{on} + E_{off})\frac{\sqrt{2}}{\pi}\left(\frac{I_{out}}{I_{rated}}\right)K_{swT\_I} \\ &\times\left(\frac{V_{cc}}{V_{rated}}\right)K_{swT\_V} \times [1 + K_{swT\_T}(125℃ - T_{j\_T})] \end{aligned} \tag{10}$$

$$\begin{aligned} P_{sw\_D} &= f_s E_{sp}\frac{\sqrt{2}}{\pi}\left(\frac{I_{out}}{I_{rated}}\right)K_{swD\_I}\left(\frac{V_{cc}}{V_{rated}}\right) \\ &\times K_{swD\_V} \times [1 + K_{swD\_T}(125℃ - T_{j\_D})] \end{aligned} \tag{11}$$

In (10) and (11), f_s is the carrier frequency; E_{on} is the single pulse switching-on loss of an IGBT under rated conditions; E_{off} is the single pulse switching-off loss of an IGBT under rated conditions; E_{sp} is the single pulse switching-off loss of a fast recovery diode under rated conditions; V_{cc} is bridge arm voltage; I_{rated} and V_{rated} are the reference current and reference voltage, respectively; K_{swT_I} is the current coefficient of the current amplitude affecting the switching loss of an IGBT; K_{swT_V} is the voltage coefficient of the bridge arm voltage affecting the switching loss of an IGBT; K_{swD_I} is the current coefficient of the current amplitude affecting the switching loss of a fast recovery diode; K_{swD_V} is the voltage coefficient of the bridge arm voltage affecting the switching loss of a fast recovery diode; K_{swT_T} is the temperature coefficient of the temperature affecting the switching loss of an IGBT; and K_{swD_T} is the temperature coefficient of the temperature affecting the switching loss of a fast recovery diode. There are certain differences among E_{on}, E_{off} and E_{sp} in the single pulse switching loss, which should be chosen reasonably.

Generally speaking, the curve of the switching loss changing withthe load current, on the basis of the test voltage at a junction temperature of 125℃, can be found in an IGBT parameter datasheet.When power devices operate with different voltages and junction temperatures, their power losses can be modified by the power function of the ratio between the actual withstanding voltage and the test voltage as well as the power function of the ratio between the actual junction temperature and the test junction temperature. Therefore, the IGBT switching on and off loss $E_{\mathrm{sw,T}}(I)$ of the single pulse power can be expressed as:

$$\begin{aligned} E_{\mathrm{sw,T}}(I) &= E_{\mathrm{on,T}}(I) + E_{\mathrm{off,T}}(I) \\ &= (A_{\mathrm{sw,T}} I^2 + B_{\mathrm{sw,T}} I + C_{\mathrm{sw,T}}) \\ &\times \left(\frac{U_{\mathrm{ce}}}{U_{\mathrm{base}}}\right)^{D_{\mathrm{sw,T}}} \left(\frac{T_{\mathrm{vj,T}}}{T_{\mathrm{base}}}\right)^{K_{\mathrm{sw,T}}} \end{aligned} \tag{12}$$

In (12), $A_{\mathrm{sw,T}}$, $B_{\mathrm{sw,T}}$ and $C_{\mathrm{sw,T}}$ are quadratic curve fitting coefficients of the switching loss changing with the current under the test conditions; $D_{\mathrm{sw,T}}$ is the correction coefficient of the test voltage U_{base}; $K_{\mathrm{sw,T}}$ is the correction coefficient of the test junction temperature T_{base} (under normal circumstances this is 125 ℃); U_{ce} is the actual withstanding voltage.

TABLE I
PARAMETERS OF WINDING ASYNCHRONOUS MOTOR

Rated power Pd (kW)	475
Stator voltage U_s (V)	6000
Stator current I_d (A)	59
Rotor voltage U_r (V)	640
Rotor current I_r (A)	435
Rated speed (r/min)	735
Power factor	0.85

TABLE II
COMPONENTS PARAMETERS OF INVERTER MAIN CIRCUIT

U_{dc}	1100 V
DC-link capacitor parameters	1800μF / 1300V
Power device parameters	Infineon, FF1400R17IE4 series
Switching frequency	2000Hz

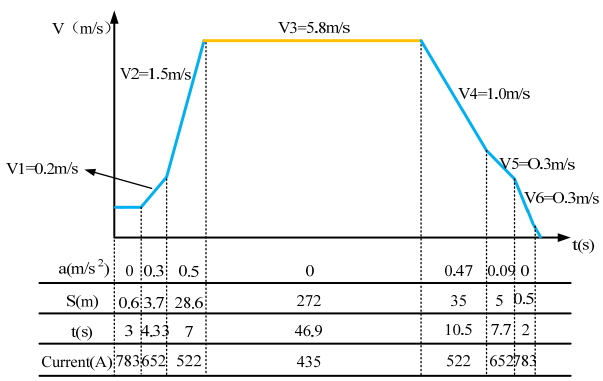

Fig. 4. Lifting conditions of one cycle of mine hoist.

The switching on loss of fast recovery diodes is very small. As a result, it can be ignored, and only the reverse recovery loss E_{sp} during the switching off should be taken into account. Therefore, the single pulse switching loss of fast recovery diodes is approximately equal to the reverse recovery loss E_{sp} .Like an IGBT, according to the parameter datasheet, the switching loss can be expressed as:

$$E_{\mathrm{rec,D}}(I) = (A_{\mathrm{rec,D}} I^2 + B_{\mathrm{rec,D}} I + C_{\mathrm{rec,D}}) \times \left(\frac{U_{\mathrm{ce}}}{U_{\mathrm{base}}}\right)^{D_{\mathrm{rec,D}}} \left(\frac{T_{\mathrm{vj,D}}}{T_{\mathrm{base}}}\right)^{K_{\mathrm{rec,D}}} \quad (13)$$

In (13), $A_{\mathrm{rec,D}}$, $B_{\mathrm{rec,D}}$ and $C_{\mathrm{rec,D}}$ are the quadratic curve fitting coefficients of the switching loss changing with a current under test conditions; $D_{\mathrm{rec,D}}$is the correction coefficient of the test voltageU_{base}; and$K_{\mathrm{rec,D}}$ is the correction coefficient of the test junction temperate T_{base}.

In view of the symmetry of both bridges in a system and

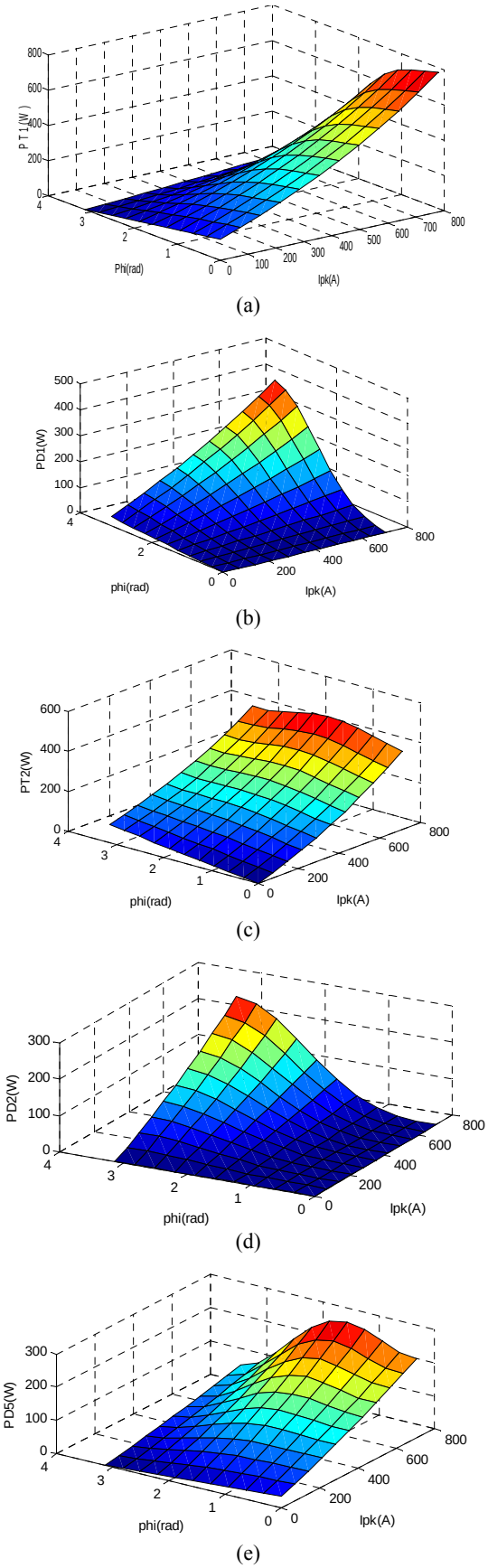

Fig. 5. Relationship among power loss, load current and load impedance angle of upper bridge arm in phase A.

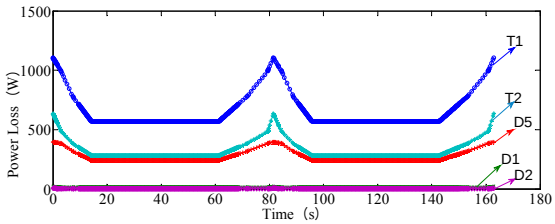

Fig. 6. Dynamic power-loss curves of the upper bridge arm in phase A.

the upper and lower arms in one bridge, the total power loss P_{TP} is equal to the sum of six half bridges, and can be defined as follows using the half bridge of phase A.

$$P_{TP} = 6 \times (P_{T\_a} + P_{D\_a}) \tag{14}$$

Therefore, the following section only calculates the power loss of the upper bridge arm of phase A in accordance with the actual parameters. The parameters of the experiment platform are as follows.

The welldepth is 348m. Meanwhile, the lifting conditions of one cycle are shown in Fig. 4.

First of all, according to the FF1400R17IE4 datasheet and the power-loss calculation theory described in the previous section, the relationship among power loss, load current and load impedance angle upper bridge arm in phase A can be obtained. This is shown in Fig. 5.

All of the dynamic power losses of the upper bridge arm in phase A can be illustrated in Fig. 6.

According to the traditional average power loss calculation of inverters in [11], the total average power loss of aNPC three-level inverter is 7380W, which acts as the total heat source during the process of the forced-air cooling system design.

III. Forced-Air Cooling System Design

The total heat source calculated in previouschapter is the reference power during the theory analysis and design of the forced-air cooling system. As noted in[23], the performance and weight of the heat sink-fan forced-air cooling system mainly depends on the parameters shown in Fig. 7.

The volume and weight of the duct and housing are always affected by many factors and have few differences under the same technological level. Therefore, they are beyond theconsideration of this paper. In addition, the heat sink material in this paper is aluminum, and the material properties including the thermal conductivity, the thermal conductivity of the air flow and the density of the heat sink material arenot considered in this paper. The parameters in TABLE III are the factors used in the cooling system design.

It can be seen from TABLE IIIthat the heat sink, duct and fan affect the cooling capacity of the whole cooling system.Meanwhile, they are the most important factors influencing the total weight and power density of aninverter.

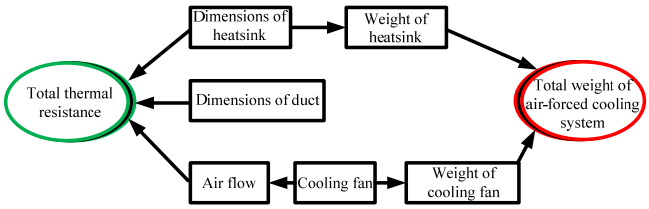

Fig. 7. Factors affecting the thermal resistance and weight of heat sink-fan air-forced cooling system.

TABLE III
Design Factors of Cooling System

	Detailed parameters
Heat sinkgeometry	Fin height, fin width, number of fins, heat sink length, baseplate thickness, channel width
Duct geometry	Duct width, duct length, duct height
Fan	Air flow curve, fan weight, dimension

Under the premise of the constant thermal conductivity of aluminum and the heat source of power devices, a methodto design the fin thickness to reduce the weight of the heat sink as much as possible and to increase the number of fins as much as possible to improve the total fin surface area plays an important role in the process of the cooling system design and optimization. It must pointed out that asignificant improvement inthe fin weight and fin width is limited by the manufacturing capacity and cost[24]. On the other hand, the cooling fan is an important factor influencing both the convection and total weight, which affects the system structure and power density. A set of air flow curves fromstandard fans available within this power range is shown in Fig. 8. Although it is not like the aspects of the fan volume, air flow, and static pressure, which have some theoretical formulas to support the design, on the basis of technical manuals and industry experience, afan with a much larger air flow rate and a much higher static pressure means a much heavier fan. Whether afan has the minimum weight and meets the demands of cooling capacity or not determinesthe thermal stability of an inverter. In addition, the longitudinal size, the total weight and most importantly the power density of the inverter are also determined by the chosen fan.

According to [25], the total thermal resistance of the whole cooling system, including the thermal resistances of the baseplate and fins, can be presented as:

$$R_{total} = \frac{b}{k \cdot L \cdot W} + \frac{1}{\frac{n}{R_{fin}} + h \cdot (n-1) \cdot s \cdot L} \tag{15}$$

where b is the baseplate thickness, k is the thermal conductivity of aluminum, L is the length of the heat sink, W is the width of the heat sink, h is the convective heat transfer coefficient, n is the number of fins, and R_{fin} is the thermal resistance of a single fin.

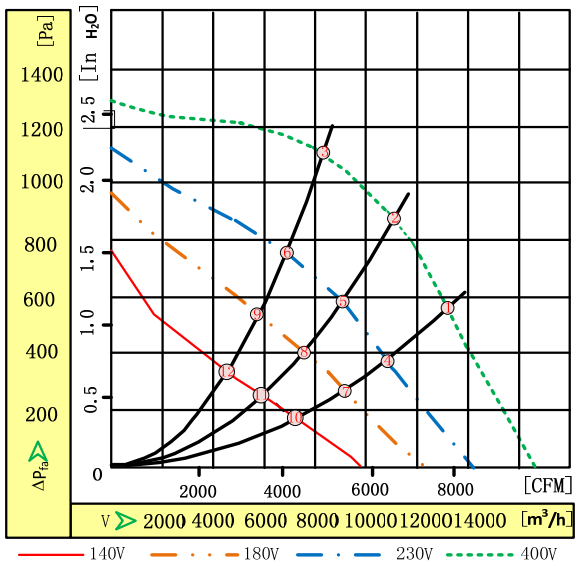

Fig. 8. Relationship curves among fan power, air flow, and static pressure.

From [9], R_{fin} can be expressed as:

$$R_{fin} = \frac{1}{\sqrt{h \cdot P_c \cdot k \cdot A_c}\tanh(m \cdot a)} \tag{16}$$

where m stands for the fin parameter, and can be expressed as follows:

$$m = \sqrt{\frac{h \cdot P_c}{k \cdot A_c}}. \tag{17}$$

In (16) and (17), P_c is the perimeter of a fin, A_c is the cross-sectional area of a fin, m is the fin parameter, and a is the height of a fin. P_c and A_c come from the following equations:

$$P_c = 2a + 2d \tag{18}$$

$$A_c = a \cdot d. \tag{19}$$

During the construction of the thermal model, the most significant parameter is h, and it can be expressed as in [17]:

$$h = \frac{Nu \cdot k_f}{s}. \tag{20}$$

In (20), k_f is the fluid thermal conductivity, and Nu is the Nusselt number, which means the ratio of the convective to the conductive heat transfer across the convection boundary. As shown in [17] by Teertstra et al., Nu can be calculated by the following equation:

$$Nu = \left[\left(\frac{Re_s^* P_r}{2}\right)^{-3} + \left(0.664\sqrt{Re_s^*}P_r^{\frac{1}{3}}\sqrt{1+\frac{3.65}{\sqrt{Re_s^*}}}\right)^{-3}\right]^{-\frac{1}{3}} \tag{21}$$

where, P_r is the Prandtl number, which stands for the ratio of the viscosity and the thermal diffusivity. Re_s^* is the adjusted channel Reynolds number, which is a one channel parameter, and can be determined from the following expression:

$$Re_s^* = \frac{Re_s \cdot s}{L}. \tag{22}$$

In (22), Re_s is the Reynolds number, which indicatesthe ratio of the inertial forces to the viscous forces, and can be presented as:

$$Re_s = \frac{s \cdot V_{ch}}{\nu}. \tag{23}$$

In this equation, s is the channel width, V_{ch} is the average channel velocity, and ν is the kinematic viscosity of air. Meanwhile, the pressure drop of the proposed heat sink proposed will be calculated from the following equation:

$$\Delta P = (f_{app} \cdot \frac{n \cdot (2a \cdot L + s \cdot L)}{a \cdot W} + K_c + K_e)\frac{\rho \cdot V_{ch}^2}{2} \tag{24}$$

where, f_{app} is the apparent friction factor for a hydrodynamically developing flow, K_c is the coefficient of a sudden contraction of the heat sink channel, K_e is the coefficient of a sudden expansion of the heat sink channel, and ρ is the air density. f_{app} for a rectangular channel can be evaluated using the following laminar flow formulation developed in [8]:

$$f_{app} = \frac{1}{\mathrm{Re}_{Dh}}\left[\left(\frac{3.44}{\sqrt{L^*}}\right)^2 + (f \cdot \mathrm{Re}_{Dh})^2\right]^2. \tag{25}$$

In (25), Re_{Dh} is the channel Reynolds number, L^* is the adjusted length of the channel, and f is the friction factor.

$$L^* = \frac{L}{D_h \mathrm{Re} D_h} \tag{26}$$

$$D_h = \frac{2 \cdot s \cdot a}{s + a} \tag{27}$$

$$\mathrm{Re} D_h = \frac{V_{ch} \cdot D_h}{\nu} \tag{28}$$

In the aforementioned equations, D_h is the hydraulic diameter of the channel. In (24), the coefficients K_c and K_e can be expressed as(from [20] and [25]):

$$K_c = 0.42\left[1 - \left(1 - \frac{n \cdot d}{W}\right)^2\right] \tag{29}$$

and:

$$K_e = \left[1 - \left(1 - \frac{n \cdot d}{W}\right)^2\right]^2. \tag{30}$$

$f \cdot Re_{Dh}$ can be expressed as:

$$f \cdot Re_{Dh} = 24 - 32.527\left(\frac{s}{a}\right) + 46.721\left(\frac{s}{a}\right)^2 - 40.829\left(\frac{s}{a}\right)^3 + 22.954\left(\frac{s}{a}\right)^4 - 6.089\left(\frac{s}{a}\right)^5 \quad (31)$$

In accordance with [13], an approximation equation to express the correlation of channel velocity and the free stream velocity with a bypass air flow in the duct can be obtained as:

$$V_{ch} = V_f\left(\frac{s+d}{s}\right)[1-(L_1 \cdot a_1)^{0.125}] \cdot \quad (32)$$

In (32), V_f is the approaching speed, L_1 is the duct dimensionless length, and a_1 is the ratio of the bypass area and the single channel area. They are defined as:

$$L_1 = \frac{L}{Re_d \cdot D_{hd}} \quad (33)$$

$$D_{hd} = \frac{2 \cdot DW \cdot DH}{DW + DH} \quad (34)$$

$$a_1 = \frac{DW \times DH}{s \cdot a} \quad (35)$$

where DW and DH are the width and height of the duct, respectively.

Generally speaking, the pressure drop in the heat sink and duct geometry is an important factor that impacts the required air pressure of the fan. In addiiton, an empirical expansion coefficient was adopted from [23] to indicate the relationship:

$$K_{e,fan} = \left[1 - \left(\frac{L^2_{fan}}{DH \cdot DW}\right)^2\right]^2 \cdot \quad (36)$$

In (36), $K_{e,fan}$ is the coefficient of a sudden air flow expansion of the fan, and L_{fan} is the length of the fan frame. It can be seen from [23] that (36) describes the air flow expansion with considerable accuracy (<10% error, analytical calculation compared with the FEA simulation results).

$$P_{\text{fan}} = \Delta P + \frac{K_{e,\text{fan}} \cdot \rho \cdot V^2_{\text{fan}}}{2} . \quad (37)$$

By putting (36) into (37) the air flow of the fan can be expressed as:

$$V_{\text{fan}} = V_f \cdot DH \cdot DW . \quad (38)$$

Both P_{fan} in (37) and V_{fan} in (38) constitute the operation point of the fan, which must be on the air flow curve. The total thermal resistance can be obtained by solving theabove equations, and the total weight of the heat sink-fan cooling system can be expressed by the following equation:

$$W_{total} = \rho_h\left(b \cdot L \cdot W + n \cdot a \cdot d \cdot L\right) + W_{\text{fan}} \quad (39)$$

where, W_{total} and W_{fan} stand for the total weight of the cooling system and the fan weight respectively.

TABLE IV
DESIGN FACTORS OF COOLING SYSTEM

Design variable	n, d, W, L, a, v_{ch}
Design target	Minimum W_{total}
Design limits	n is integer, $n > 1$ $DW > d > 1\text{mm}$ $DW > W > W_m$ $DL > L > L_m$ $DW > s > 1\text{mm}$ $DH > s > 1\text{mm}$ $DH > a > 0$ $V_{ch} > 0$ $R_{total} < (T_c - T_a)/P$ P_{fan} and V_{fan} should be on fan curve

TABLE V
CASE STUDY PARAMETERS

Item	Description
Power module	Total average power loss: 7380W
Heat sink material	Junction temperature:125℃
Ambient temperature	Aluminum (200W/m-k) 30℃

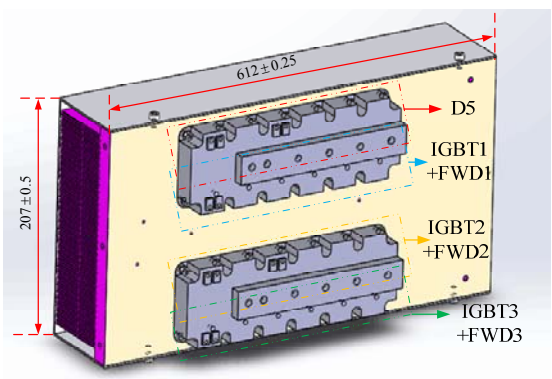

Fig. 9. The ideal heat sink structure and distribution of IGBTs based on the total average power loss

By putting the total power loss into the above equations as a heat source, the ideal heat sink structure and the distribution of the IGBTs can be obtained as shown in Fig. 9.

In Fig. 9 IGBT3+FWD3 is the power device of the lower bridge arm of phase A. Put the average power loss of each power device in accordance with the dynamic power loss curve shown in Fig.6 into this distribution, and it can be determined that the upper IGBT total power loss is 905W and that the lower IGBT total power loss is 970W.

TABLE VI
PARAMETERS OF HEAT SINK

Material	Aluminum (210W/m-k)
N (number of fins)	28
W (width of heat sink mm)	207 ± 0.5
L (length of heat sink mm)	612 ± 0.25
s (spacing between two fins mm)	6.5
a (height of fin mm)	101 ± 0.15

TABLE VII
PARAMETERS OF FAN

Phase	3
Nominal voltage [V]	400
Connection	Y
Frequency[Hz]	50
Speed[min^{-1}]	1375
Power input[W]	1430
Back pressure[Pa]	0
Air flow[m^3/h]	8320
Sound pressure level[dB(A)]	78

Put the total average power loss into the cooling system design, and the pressure drop between the inlet and outlet of the heat sink can be obtained as follows:

$$\Delta P=1075.78\,\text{Pa}$$

The approaching speed should meet the following requirement:

$$V_f > 8.5\text{m/s}$$

Based on these two parameters, search for a fan according to the operation point shown in Fig.8, and the fan with working characteristics at point ③can be used in this design. The detailed parameters of this fan are shown in TABLE VII.

IV. SIMULATION AND EXPERIMENT

The dynamic junction temperature curves of all of the power devices in the upper bridge arm of phase A for two cycles was generated from the online thermal simulation tool of the Infineon website, and is shown in Fig. 10.

Using finite element analysis software ANSYS to carry out athermal analysis of the cooling system, the simulation results are as follows.

It can be seen from Fig. 11 that the highest junction temperature (76.1℃) of power devices is under the maximum temperature (125℃) of a FF1400R17IE4 under normal working conditions. In addition, the inlet wind speed of the heat sink is much larger than 8.5 m/s, and the pressure drop between the inlet and outlet of the heat sink(the outlet is connectedto the negative pressure cavity, which can be considered as the 0 Pa reference point) is 1174Pa, which is close to the theoretical analysis result $\Delta P=1075.78$ Pa.

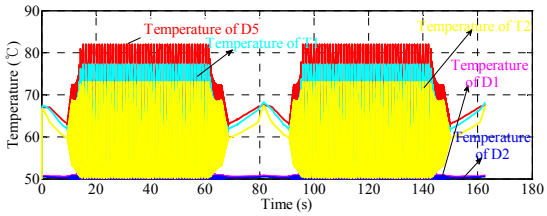

Fig. 10. Junction temperature dynamic curves of phase A based on average power losses.

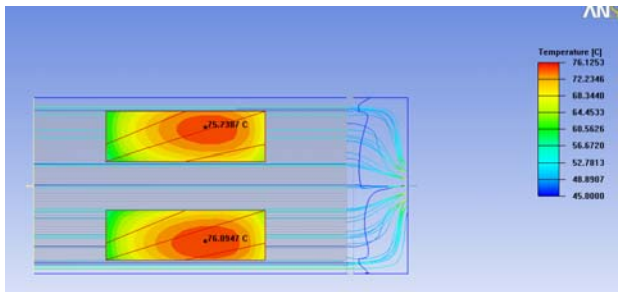

(a)

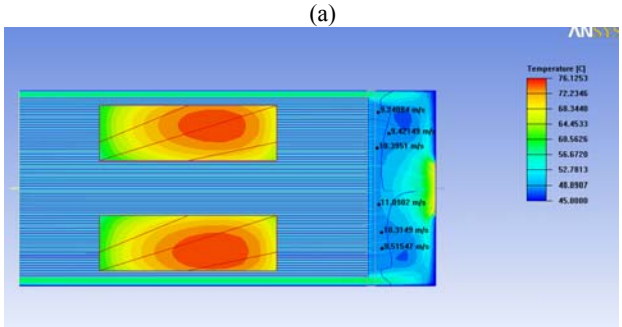

(b)

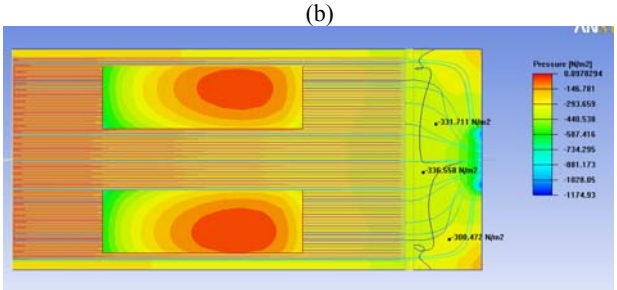

(c)

Fig. 11. Steady-state thermal simulation of the upper bridge arm of phase A in NPC three-level inverter. (a) Temperatures of power devices; (b) Inlet wind speed of heat sink; (c) Inlet pressure of heat sink.

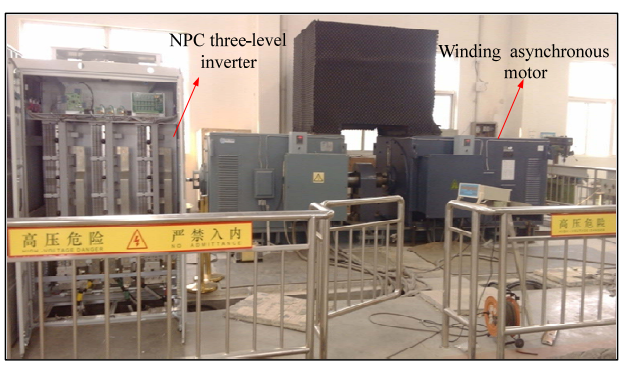

Fig. 12. The 1 MW experiment platform.

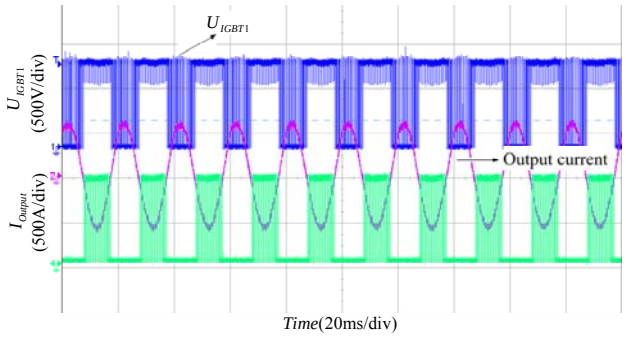

Fig. 13. Waveforms of steady-state operation of inverter.

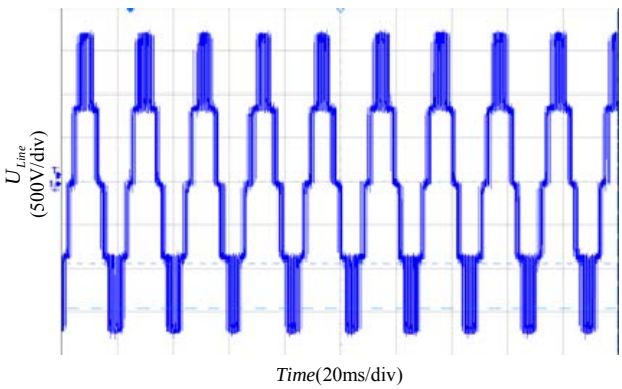

Fig. 14. Line Voltage Waveform of steady-state operation.

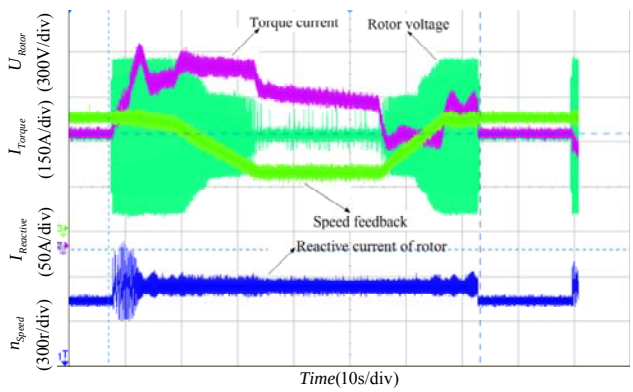

Fig. 15. Waveforms of Mine Hoist operating in one cycle.

All of the simulations show that the proposed heat sink and fan model built based on the average power loss acting as a heat source is suitable for aninverter to work in one cycle.

The experiment platform is shown in Fig. 12. In order to simulate the real working conditions of ahoist, the temperature rise experiment of multicycle lifting is made on this platform in accordance with the lifting conditions of one cycle, as shown in Fig. 4, and the duration is 1 hour. The experiment results are as follows.

It can be seen from Fig. 13, Fig. 14, and Fig. 15 that the system operates safely in one cycle with large currents in the startup and deceleration stages. The wind speed of the heat sink inlet during the process of system operation under normal conditions is shown in Fig. 16, and the actual speed is 9.86m/s, which is larger than the theoretical value of 8.5m/s. The initial temperature of the inverter is the ambient

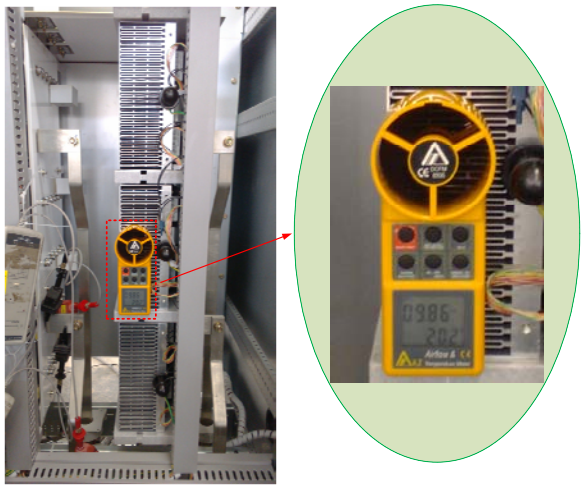

Fig. 16. Wind speed of heat sink inlet.

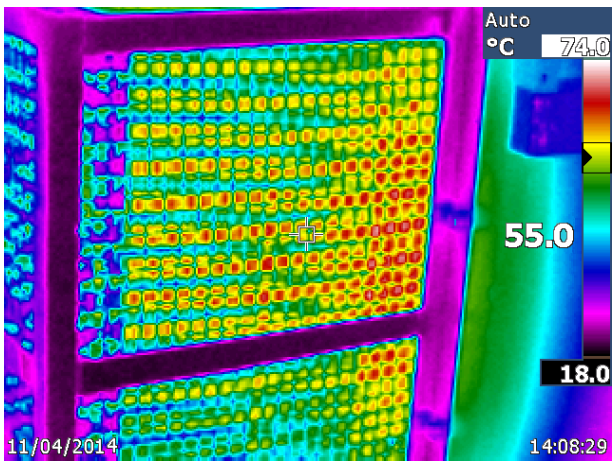

(a) Substrate temperature.

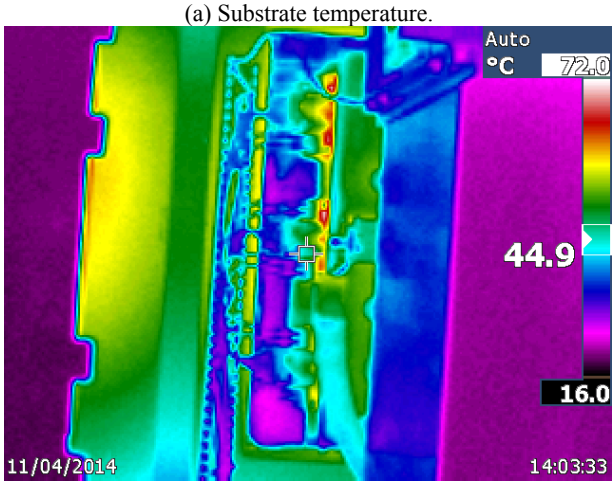

(b) Surface temperature of power devices.

Fig. 17. Temperatures of the upper bridge arm of phase A at constant speed period.

temperature. After several lifting cycles the temperature keeps a dynamic balance at a certain temperature level, which includes a rapid temperature climb at the startup and deceleration stages, and a gradual decrease during the constant speed period. It can be seen from Fig. 17 that the temperature of the heat sink substrate fluctuates around 72℃

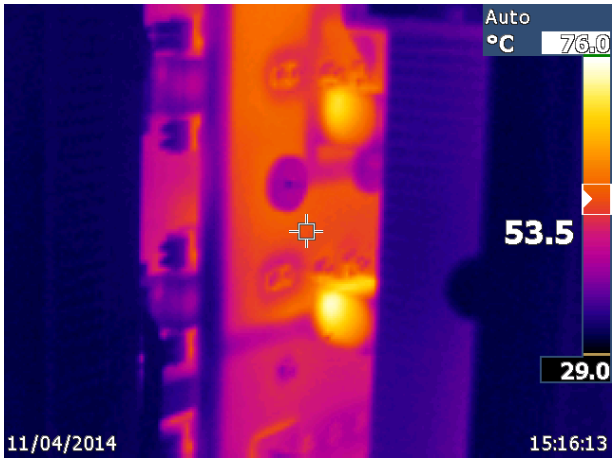

(a) Temperature of bridge arm back of phase A.

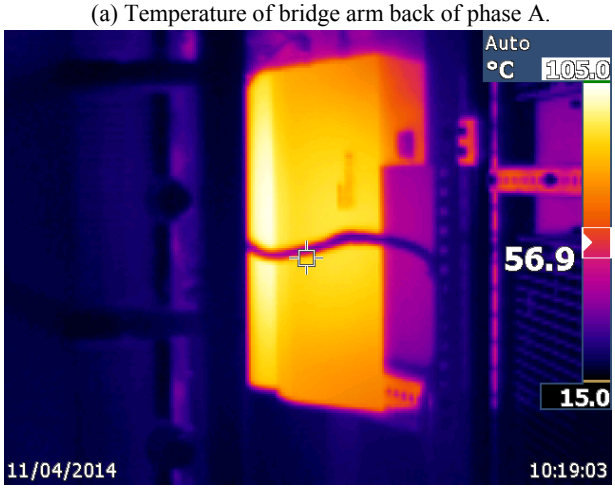

(b) Surface temperature of T2.

Fig. 18. Temperatures of bridge arm back and T2 of phase A at startup and deceleration stages.

Fig. 19. Damage anatomy of power device caused by heat accumulation.

TABLE VIII
PARAMETERS OF OPTIMIZED HEAT SINK

Material	Aluminum (210W/m-k)
N (Number of fins)	48
W (width of heat sink mm)	360 ± 0.5
L (length of heat sink mm)	612 ± 0.25
s （spacing between two fins mm）	6.5
a （height of fin mm）	101 ± 0.15

isothermal up and down within 2 ℃ .Meanwhile, the maximum surface temperature of the power devices is 72℃. The temperature of bridge arm back of phase A, shown in Fig. 18, indicates that the area with the highest temperature is the location of the lower IGBT of phase A. It can be seen that its maximum surface temperature reached approximately 105℃. It can be deduced, based on engineering experience, that the junction temperature is close to the maximum allowable temperature 125 ℃, which was confirmed by the heat accumulation damage of T2 at the 45th minute. The anatomy of T2 is shown in Fig. 19.

From the analyses above, it can be concluded that undera heavy load with periodic operation, using the average power loss as aheat source to design the cooling system is not suitable for systemsoperating in the continuous multicycle state with a frequent overload. The reason is that using the average power loss as a heat source means spreading the total power loss of the power devices in one cycle on average. Thiscoversspecial ranges generating large power losses in a short period of time. During the multicycle operation,heat accumulates gradually and eventuallydamages the power devices. In mine hoist systems, the special ranges are the deceleration period of the former cycle and the acceleration period of the next period. This is due to the fact that the heat generated in the deceleration period isaccumulate to the next cycle's accumulation, which exceeds the thermal capacity of the cooling system and becomesa potential threat to the power devices. Both of the ranges constitute the maximum power-loss range.According to the dynamic power-loss curves,the average power losses of all power devices are extracted as the correction power to optimize the cooling system. From the above simulation and experimental results, it can be found that the total power of the fan is enough for this inverter and all that needs to be doneright now is to optimize the size and shape of the heat sinks within the requirements of the theoretical analysis to keep a higher power density. The optimization results are as follows.

The heat sink model shown in Fig. 20 is different from the model in Fig. 1 and Fig. 9 in some aspects including the fact that the heat sink number of one bridge arm changes from 3to 2, all the power devices are distributed in one heat sink, the width of each heat sink increases by 153mm, and the number

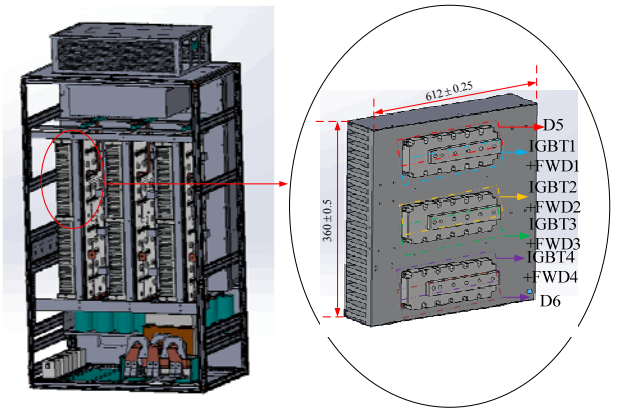

Fig. 20. The heat sink structure and distribution of power devices after optimization.

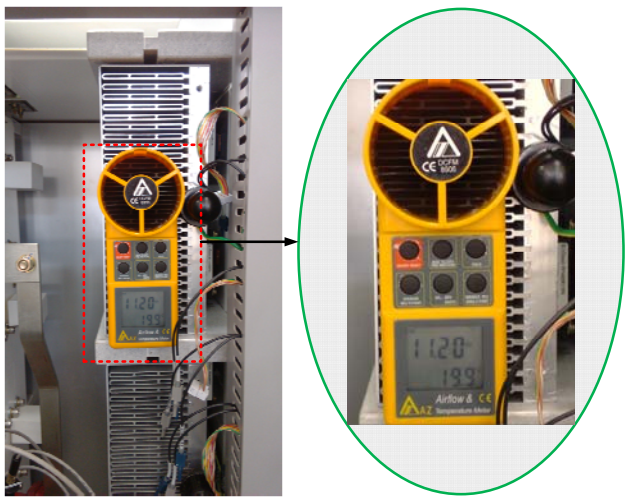

Fig. 21. The wind speed of optimized heat sink.

of fins in one heat sink increase by 12. It can be determinedthat the pressure of the heat sink inlet increase by 14.3% compared with the old one.The experiment results are as follows.

It can be seen from Fig. 21 and Fig. 22 that the inlet wind speed of the optimized heat sink is 11.20 m/s, which is a 13.5% increase in rate compared with the former heat sink; the maximum temperature of the optimized heat sink is 62℃, which is a 16.2% decrease in rate compared with the former heat sink; the maximum temperature of the T1 module surface is 71℃, which is a 6.6% decrease compared with the former one; and the maximum instantaneous temperature of the T2 module surface at startup and deceleration stages is 68℃, which is a 35.2% decrease compared with the former one. From the results comparison, it can be concluded that whenthe fin number of the optimized heat sink increases, the wind resistance is decreased, the pressure drop between the inlet and outlet of the heat sink is enhanced, which improves the wind speed, and finally the heat capacity is upgraded. The experiment results show that T2 has the largest temperature reduction and can operate safely during the whole temperature rise test, which verifies that the optimization

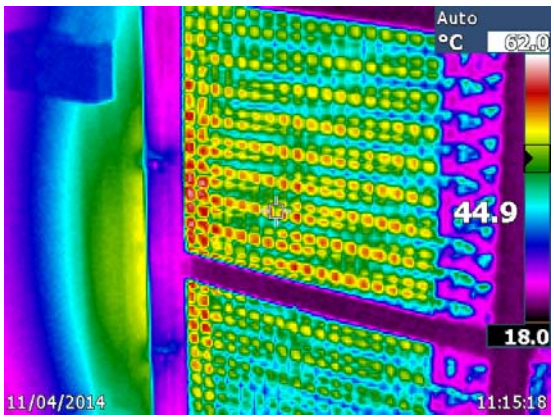

(a) Substrate temperature.

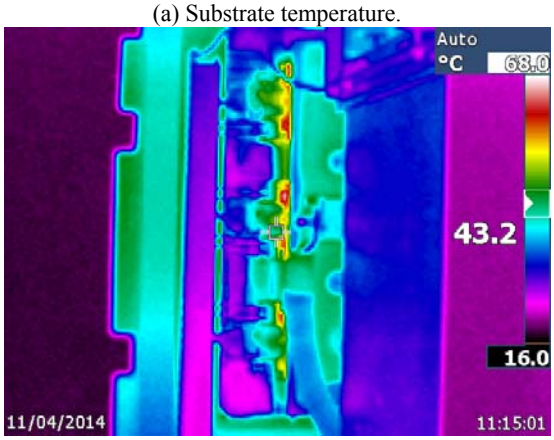

(b) Surface temperature of power devices.

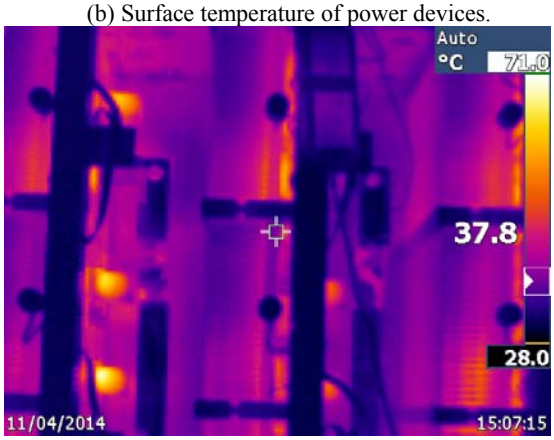

(c) Temperature of bridge arm back of phase A.

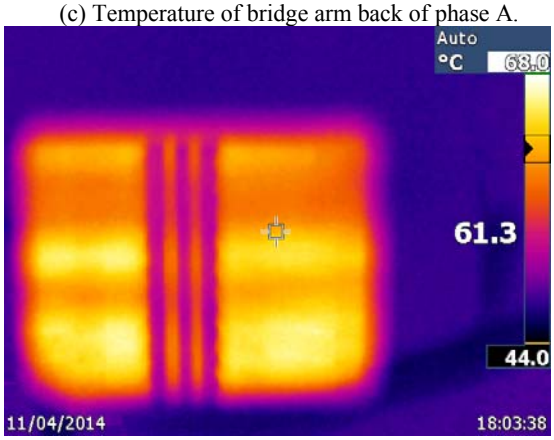

(d) Surface temperature of T2.

Fig. 22. The experiment results after optimization.

design of the cooling system based on the dynamic power loss calculation of the maximum power-loss range is both effective and feasible.

V. CONCLUSION

In this paper, the average power losses of a 1MW mine hoist were calculated withthe fast power-loss calculation method considered as aheat source to design the cooling system. Based on theoretical analyses, the forced-air cooling system model was designed, and it was verifiedby simulation. However,as a multicycle load, the system has a weakness in terms of instantaneous heat accumulation after continuous overload operation. Finally, according to ananalysis of the periodic working conditions, the maximum power-loss range was obtained and its dynamic power loss was taken into the optimized cooling system model as aheat source to preventinstantaneous heat accumulation. The effectiveness and feasibility of optimized design for a NPC three-level inverter cooling system based on the dynamic power loss calculation of the maximum power-loss range was verifiedby experimental results.

ACKNOWLEDGMENT

The authors would like to thank 2014 Jiangsu Province Natural Science Foundation (BK20140204), the Research and Innovation Program of Postgraduates in Jiangsu Province (CXZZ13_0930) and the Fundamental Research Funds for the Central Universities(2012LWB73).

REFERENCES

[1] P. M. Fabis, D. Shum, and H. Windischmann, "Thermal modeling of diamond-based power electronics packaging," in *15th Annual IEEE Semiconductor Thermal Measurement & Management Symposium*, pp. 98-104, Mar. 1999.

[2] P. Mao, S. J. Xie, and Z. G. Xu, "Switching transients model and loss analysis of IGBT module," *Proceedings of the CSEE*, Vol. 30, No. 15, pp. 40-47, 2010.

[3] D. Yi and M. Y. Liao, "Losses calculation of IGBT module and heat dissipation system design of inverters," *Electric Drive Automation*, Vol. 24, No. 3, pp. 159-163, 2011.

[4] A. D. Rajapakse, A. M. Gole, and P. L. Wilson, "Electromagnetic transients simulation models for accurate representation of switching losses and thermal performance in power electronic systems," *IEEE Trans. Power Del.*, Vol. 20, No. 1 , pp. 319-327, Jan. 2005.

[5] F. Krismer and J. W. Kolar, "Accurate power loss model derivation of a high-current dual active bridge converter for an automotive application," *IEEE Trans. Ind. Electron.*, Vol. 57, No. 3, pp. 881-891, Mar. 2010.

[6] Q. Chen, Q. Wang, W. Jiang, and C. Hu, "Analysis of switching losses in diode-clamped three-level converter," *Transactions of China Electrotechnical Society*, Vol. 32, No. 2, pp. 68-75, Feb. 2008.

[7] M. H. Bierhoff and F. W. Fuchs, "Semiconductor losses in voltage source and current source IGBT converters based on analytical derivation," in *IEEE 35th Annual Power Electronics Specialists Conference*, Vol. 4, pp. 2836-2842, 2004.

[8] T. J. Kim, D. W. Kang, Y. H. Lee, and D. S. Hyun, "The analysis of conduction and switching losses in multi-level inverter system," in *IEEE 32nd Annual Power Electronics Specialists Conference*, Vol. 3, pp. 1363-1368, 2001.

[9] Q. J. Wang, Q. Chen, W. D. Jiang, and C. G. Hu, "Analysis of conduction losses in neutral-point-clamped three-level inverter," *Transactions of China Electrotechnical Society*, Vol. 22, No. 3, pp. 66-70, Mar. 2007.

[10] S. Dieckerhoff, S. Bernet, and D. Krug, "Power loss-oriented evaluation of high voltage IGBTs and multilevel converters in transformerless traction applications," *IEEE Trans. Power Electron.*, Vol. 20, No. 6, pp. 1328-1336, Nov. 2005.

[11] W. Jing, G. J. Tan, and Z. B. Ye, "Losses calculation and heat dissipation analysis of high-power three-level converters," *Transactions of China Electrotechnical Society*, Vol. 26, No. 2, pp. 134-140, Feb. 2011.

[12] K. Ma, Y. Yang, and F. Blaabjerg, "Transient modelling of loss and thermal dynamics in power semiconductor devices," in *IEEE Energy Conversion Congress and Exposition (ECCE)*, pp. 5495-5501, Sep. 2014.

[13] W. Jing, *Study on power device losses of high-power three-level converter*, Ph. D. Dissertation, China University of Mining and Technology, China, 2011.

[14] J. h. Hu, J. G. Li, and J. B. Zou, "Losses calculation of IGBT module and heat dissipation system design of inverters," *Transactions of China Electrotechnical Society*, Vol. 24, No. 3, pp. 159-163, Mar. 2009.

[15] F. Hong, R. Z. Shan, H. Z. Wang, and Y. G. Yan, "Analysis and calculation of inverter power loss," *Proceedings of the CSEE*, Vol. 28, No. 15, pp. 72-78, 2008.

[16] X. He, Y. Wu, H. Luo, P. Li, and W. Li, "Quasi-online modeling method of the power inverter losses based on igbt offline test platform," *Transactions of China Electrotechnical Society*, Vol. 29, No. 6, pp. 1-6, Jun. 2014.

[17] U. Drofenik, G. Laimer, J. W. Kolar, "Theoretical converter power density limits for forced convection cooling," in *Proceedings of the PCIM*, pp. 608-619, 2005.

[18] U. Drofenik and J. W. Kolar, "Analyzing the theoretical limits of forced air-cooling by employing advanced composite materials with thermal conductivities>400 W/mK," in *4th International Conference on Integrated Power Systems (CIPS)*, pp. 1-6, Jun. 2006.

[19] E. M. Sparrow, B. R. Baliga, and S. V. Patankar, "Forced convection heat transfer from a shrouded fin array with and without tip clearance," *Journal of Heat Transfer*, Vol. 100, No. 4, pp. 572-579, Nov. 1978.

[20] S. Lee, "Optimum design and selection of heat sinks," in *11th Annual IEEE Semiconductor Thermal Measurement and Management Symposium*, pp. 48-54, Feb. 1995.

[21] W. Leonard, P. Teertstra, J. R. Culham, and A. Zaghol, "Characterization of heat sink flow bypass in plate fin heat sinks," in *ASME International Mechanical Engineering Congress and Exposition*, pp. 189-196, Nov. 2002.

[22] R. Hossain, J. R. Culham, and M. M. Yovanovich, "Influence of bypass on flow through plate fin heat sinks," in *23rd Annual IEEE Semiconductor Thermal Measurement and Management Symposium*, pp. 220-227, Mar. 2007.

[23] P. Q. Ning, F. Wang, and K. D. T. Ngo, "Forced-air cooling system design under weight constraint for high-temperature SiC converter," *IEEE Trans. Power Electron.*, Vol. 4, No. 29, pp. 1998-2007, Apr. 2014.

[24] R. A. Wirtz, W. Chen, and R. Zhou, "Effect of flow bypass on the performance of longitudinal fin heat sinks," *Journal of Electronic Packaging*, Vol. 116, No. 3, pp. 206-211, Sep. 1994.
[25] J. R. Culham and Y. S. Muzychka, "Optimization of plate fin heat sinks using entropy generation minimization," *IEEE Trans. Compon. Packag. Technol.*, Vol. 24, No. 2, pp. 159-165, Jun. 2001.

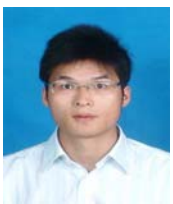

Shi-Zhou Xu was born in Henan Province, China, in 1985. He received his B.S. degree in Electrical Engineering from the Henan University of Urban Construction, Pingdingshan, China, in 2009; and his M.S. degree in Electrical Engineering from the China University of Mining and Technology, Xuzhou, China, in 2012. He is presently working towards his Ph.D. degree in Electrical Engineering in the Department of Information and Electrical Engineering, China University of Mining and Technology. His current research interests include cooling system optimization, laminated busbar research, and high-power three-level inverter modeling, control and improvement.

Feng-You He was born in Zhangjiakou, Hebei, China, in 1963. He received hisB.S. degree inAutomation from the China University of Mining and Technology, Xuzhou, China, in 1984; and his M.S. and Ph.D. degrees inPower Electronics and Drives from the China University of Mining and Technology, in 1992 and 1995, respectively. Since 1984, he has been with the Department of Information and Electrical Engineering, China University of Mining and Technology, where he is presently working asa Professor. His current research interests include the improvement of inverters, the advanced control of electrical machines, and power electronics.